Donor-Stabilized Silyl Cations. 12.[1] Electrochemical Evidence for Ionic Dissociation of Hexacoordinate Silicon Complexes

Viatcheslav Jouikov,*,† Boris Gostevskii,‡ Inna Kalikhman,‡ and Daniel Kost‡

Laboratory of Molecular and Macromolecular Electrochemistry, UMR 6510, SESO, University of Rennes I, 35042 Rennes, France, and Department of Chemistry, Ben Gurion University of the Negev, Beer Sheva 84105, Israel

Received July 10, 2007

Molar conductivities (Λ_m) were measured for four formally hexacoordinate silicon dichelates (**1**−**4**) in CH_2Cl_2, to support previous NMR evidence suggesting ionic dissociation. Concentration dependence of the conductivities at constant temperature revealed substantial ionic conductivity and ion-pair formation in **2** and **3**, lower (kinetically controlled) conductivity of **1**, and practically no ionic dissociation of **4**. Temperature dependence of the molar conductivities shows an increase of Λ_m of **2** and **3** with increasing temperature, resulting from the decrease in solvent viscosity, as expected from a fully ionic solute. In contrast, the conductivities of **1** and **4** *decrease* as the temperature is increased, indicating chemical control of ion concentration: decrease in ionic dissociation and predominance of the hexacoordinate silicon form as the temperature is increased. These results are in full agreement with previous ^{29}Si NMR measurements: complexes with either bulky (**3**) or very good leaving groups (**2**) as monodentate ligands are essentially fully ionic at room temperature; those with poorer leaving groups or highly electron withdrawing ligands (**1**, **4**) tend to resist dissociation, and the extent of dissociation increases as the temperature is lowered.

Introduction

Hexacoordinate halogeno-silicon dichelates undergo equilibrium ionic dissociation to pentacoordinate siliconium halides (eq 1), driven by hydrogen bond donor solvents, such as dichloromethane, chloroform, and fluorodichloromethane.[2] The equilibrium population ratio is strongly temperature dependent, with ionization increasing as the temperature decreases, presumably due to intense ion solvation at lower temperatures. Evidence for ionization was obtained from ^{29}Si NMR spectra (substantial downfield shift of the resonance), as well as by direct observation in single-crystal X-ray analysis of a siliconium triflate that featured a well-separated cation and anion in the solid state.[2] However, no direct evidence for the existence of *free* siliconium ions in solution could be offered, and the state of ion pairs (tight, solvent-separated, or free) remained unknown. The present paper describes the study of ionization of four different hexacoordinate silicon complexes, **1**−**4**, by means of conductimetry and cyclic voltammetry (CV), providing further evidence for the existence of free ions in some of the compounds in solution. The results of the conductivity measurements presented herein are in excellent agreement with the reported ^{29}Si NMR results.[2]

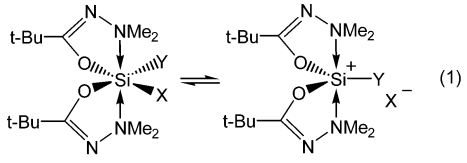

(1)

1, X = Cl, Y = Me
2, X = OSO_2CF_3, Y = Me
3, X = Cl, Y = t-Bu
4, X = Y = Cl

† University of Rennes.
‡ Ben-Gurion University.

Conductimetry was chosen as a method directly allowing the assessment of the state of ionization in solutions. The ionic state in aqueous solutions and polar organic solvents is usually well described by classical Debye−Hückel−Onsager theory.[3] However, exploiting conductivity data in low-ϵ media is a more delicate task, because of substantially shortened Coulombic distances promoting the formation of ion pairs and complex ion aggregates, driven by distance-dependent forces. This is also due to the lack of a general comprehensive theory of conductivity as pointed out previously.[4a] Triple and higher ion models,[4b] their later developments considering long-range interactions in solutions,[3f−h,4a] and modification of dielectric properties of media in the vicinity of charged species[4c] are evoked for the interpretation of conductivity data. This method was successfully used for the study of conductivity and ionic association of tertiary

(1) Gostevskii, B.; Zamstein, N.; Korlyukov, A. A.; Baukov, Y. I.; Botoshansky, M.; Kaftory, M.; Kocher, N.; Stalke, D.; Kalikhman, I.; Kost, D. *Organometallics* **2006**, *25*, 5416−5423.

(2) (a) Kingston, V.; Gostevskii, B.; Kalikhman, I.; Kost, D. *Chem. Commun.* **2001**, 1272−1273. (b) Kost, D.; Kingston, V.; Gostevskii, B.; Ellern, A.; Stalke, D.; Walfort, B.; Kalikhman, I. *Organometallics* **2002**, *21*, 2293−2305.

(3) (a) Bockris, J. O'M.; Reddy, A. K. N. *Modern Electrochemistry 1, Ionics*, 2nd ed.; Plenum Press: New York, 1998; p 769. (b) Leaist, D. G. Diffusion and ionic conduction in liquids. In *Encyclopedia of Applied Physics*; Trigg, G. L., Ed.; VCH: New York, 1993; Vol. 5, p 661. (c) Murrell, J. N.; Jenkins, A. D. *Properties of Liquids and Solutions;* Wiley-Interscience: New York, 1994. (d) Antropov, L. I. *Theoretical Electrochemistry*; Vysshaya Shkola: Moscow, 1975. (e) Fuoss, R. M.; Onsager, L. *J. Phys. Chem.* **1957**, *5*, 668−682. (f) Fuoss, R. M.; Hsia, K. L. *Proc. Natl. Acad. Sci. U.S.A.* **1967**, *57*, 1550−1557. (g) Fuoss, R. M.; Onsager, L.; Skinner, J. F. *J. Phys. Chem.* **1965**, *8*, 2581−2594. (h) Barthel, J. *Angew. Chem., Int. Ed. Engl.* **1968**, *7*, 260−277. (j) Robinson, R. A.; Stokes, R. H. *Electrolyte Solutions*; Butterworth: London, 1970. (i) Smedley, S. J. *The Interpretation of Ionic Conductivity in Liquids*; Plenum Press: New York, 1980, p 195. (k) Eger, E., Zalkind, I. A., Eds. *Measurement Methods in Electrochemistry*, Vol. 2 (Russ. transl.); Mir: Moscow, 1977.

(4) (a) Barthel, J. M. G.; Krienke, H.; Kunz, W. *Physical Chemistry of Electrolyte Solutions*; Springer: Darmstadt, 1998. (b) Fuoss, R. M.; Kraus, C. A. *J. Am. Chem. Soc.* **1933**, *55*, 2387−2399. (c) Grigo, M. *J. Solution Chem.* **1982**, *8*, 529−537.

10.1021/om700687s CCC: $37.00 © 2007 American Chemical Society
Publication on Web 10/24/2007

ammonium,[5a,b] phosphonium,[5,6] and arsonium, sulfonium, and iodonium salts[5b] in organic solvents and also for the study of reactive species such as carbocations[7] and carbanions.[8] Applied to silicon derivatives, conductivity measurement was mentioned in connection with the ionic nature of (O,S,P)-donor-ligand-stabilized pentacoordinated silicenium triflates,[9] for the study of reactivity of pentacoordinated silicon species toward 2-chloroethanol,[10] and for the study of pentacoordinated silicon species obtained from complexation of triorganosilanes with semicarbazones.[11] It was also used to probe the formation of silicenium ions in solution[12] and to prove the absence of these cations or of hypervalent silicon species in the reactions of alkoxysilanes and Ph_4Si with 100% H_2SO_4.[13]

In this work, we report a conductimetry and cyclic voltammetry study aiming to elucidate the nature of species formed by silicon dichelates with intramolecular N→Si←N coordination in dichloromethane solution and the dynamic equilibrium between penta- and hexacoordinated silicon species previously investigated by ^{29}Si NMR on compounds of this family.[1,14]

Conductivity Measurements

To provide insight into intramolecular interactions in dichelates **1**−**4** and to determine their state in organic solutions, corresponding equivalent (κ) and molar ($\Lambda_m = \kappa/C$) conductivities have been determined in CH_2Cl_2 in a wide range of concentrations.

Other conditions being equal, the conductivities of **2** and **3** are about 5−8 times greater than those of the electrochemical supporting salts Bu_4NBF_4 and Bu_4PBr in 1,2-dichloro-1,1-difluoroethane[15] or of Bu_4N picrate in dichloroethane,[16] but are substantially lower for **1** and **4**. The concentration dependence of Λ_m for dichelates **1**−**3** shows a minimum (Figure 1), the appearance of which in low-polar media is traditionally related to ion-pair formation.[4b,16,17] These minima ($C_{min} \cong 3-21$ mmol L^{-1}) fall in the range where similar phenomena were observed for tetraalkylammonium salts in solvents with $\epsilon \cong 9$[15,16] and correspond to Walden's dilution for low-polar media, $\epsilon(1/C_{min})^{1/3} \cong 30$.[18] For CH_2Cl_2 ($\epsilon = 8.93$), it gives $C_{min} \cong 26$ mmol L^{-1}, which defines dichelates **1**−**3** as good ionophores.

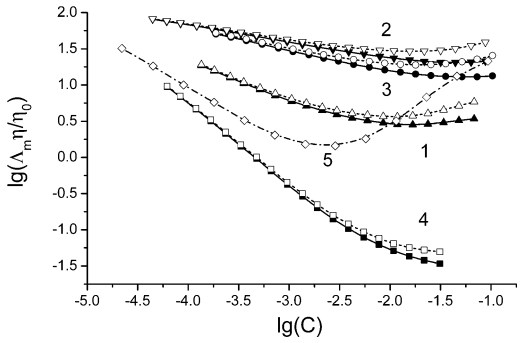

Figure 1. (1−4) Molar conductivities of compounds **1**−**4** (solid lines, $\eta/\eta_o = 1$) and Λ_m corrected for the variation of viscosity with the concentration of dissolved dichelate (dotted lines). (5) Conductivity of **2** in CH_2Cl_2 containing $\sim 5 \times 10^{-4}$ M water.

The measured values cover a large span of concentrations, so the obtained molar conductivities were corrected to the variation of solution viscosity (η) with the concentration of dichelate, accounted for through the Jones−Dole equation[19] with the leading term, A_η, obtained for each dichelate from the Falkenhagen equation[20] and $B_\eta = 1.296$.[17] The plots with new coordinates $\Lambda_m(\eta/\eta_o)-C$ reveal clearer shaped minima that are slightly shifted to lower concentrations (Figure 1).

In low-ϵ media, the activity coefficients f of free ions drop sharply when C increases from $C = 0$, so the appropriate correction has been applied to the Λ_m-C plots. Using the second approach of the Debye−Hückel theory,[21] an initial guess of f was obtained that was then adjusted (with a as fitting parameter) through the iterative procedure described by Fuoss for ion-pair dissociation.[25] The f value was retained when for two consecutive iterations the $f_n - f_{n-1} < 0.0001$ condition was fulfilled. Both η and f-corrections result in lowering C_{min}, which agrees with both the trivial[4b] and advanced[26] models of conductivity predicting the same trend in Λ_{min}.

For ionizing dichelates, one can draw a square scheme (Figure 2) involving two ionic ($K^i_{6/5}$ and $K^i_{5/4}$) and two nonionic ($K_{6/5}$ and $K_{5/4}$) dissociations.[14b,d] These equilibriums are temperature dependent, such that $K^i_{6/5}$ and $K_{6/5}$ shift clockwise[14c] and the

(5) (a) Maletin, Y. A.; Mironova, A.; Koval, B.; Danilin, V. V. *Ukr. Khim. Zhurn.* **2001**, *67*, 6−8. (b) Kline, E. R.; Kraus, C. A. *J. Am. Chem. Soc.* **1947**, *69*, 814−816. (c) Fidler, A.; Vretal, J. *Coll. Czech. Chem. Commun.* **1970**, *35*, 1905−1912.

(6) (a) Tsentovskii, V. M.; Barabanov, V. P.; Kharisova, F. M.; Busygina, T. A. *Z. Obshch. Khim.* **1971**, *41*, 1659−1662. (b) Maijs, L.; Lukevica, O. *Latv. PSR Zinatnu Akad. Vestis, Kim. Ser.* **1977**, *6*, 700−706. (c) Schiavo, S.; Marrosu, G. *Z. Phys. Chem.* **1977**, *105*, 157−172.

(7) (a) Tilley, L. J. Indiana Univ., Bloomington, IN, Avail. Univ. Microfilms Int., Order No. DA9637576. 1996, 410 pp. (*Diss. Abstr. Int., B* **1997**, *57*, 4407). (b) Kitagawa, T.; Tanaka, T.; Murakita, H.; Nishikawa, A.; Takeuchi, K. *Tetrahedron* **2001**, *57*, 3537−3547.

(8) (a) Alvarino, J. M. *J. Organomet. Chem.* **1975**, *90*, 133−138. (b) Smid, J. *Polym. Prep.* **1968**, *9*, 1063−1066. (c) Ue, M. *J. Electrochem. Soc.* **1996**, *143*, L270−L272. (d) Khan, I. M.; Hogen-Esch, T. E. *J. Polymer Sci., Part A: Polym. Chem.* **1988**, *26*, 2553−2559. (e) Solov'yanov, A. A.; Dem'yanov, P. I.; Beletskaya, I. P.; Reutov, O. A. *Zh. Org. Khim.* **1976**, *12*, 725−732.

(9) Berlekamp, U.-H.; Jutzi, P.; Mix, A.; Neumann, B.; Stammler, H.-G.; Schoeller, W. W. *Angew. Chem., Int. Ed.* **1999**, *38*, 2048−2050.

(10) Song, J.; Xu, J.; Liang, S. *Huaxue Shijie* **2004**, *45*, 342−343, 347 (CAN 145:505509).

(11) Saxena C.; Singh, R. V. *Synth. React. Inorg. Metal-Org. Chem.* **1992**, *22*, 1061−1072.

(12) (a) Lambert, J. B.; Kania, L.; Schilf, W.; McConnell, J. A. *Organometallics* **1991**, *10*, 2578−2584. (b) Lambert, J. B.; Schulz, W. J., Jr.; McConnell, J. A.; Schilf, W. *J. Am. Chem. Soc.* **1988**, *110*, 2201−2210.

(13) Flowers, R. H.; Gillespie, R. J.; Robinson, E. A. *Can. J. Chem.* **1963**, *41*, 2464−2471.

(14) (a) Sivaramakrishna, A.; Kalikhman, I.; Kerstnus, E.; Korlyukov, A. A.; Kost, D. *Organometallics* **2006**, *25*, 3665−3669. (b) Kalikhman, I.; Gostevskii, B.; Botoshansky, M.; Kaftory, M.; Tessier, C. A.; Panzner, M. J.; Youngs, W. J.; Kost, D. *Organometallics* **2006**, *25*, 1252−1258. (c) Kalikhman, I.; Gostevskii, B.; Pestunovich, V.; Kocher, N.; Stalke, D.; Kost, D. *ARKIVOC* **2006**, *5*, 63−77. (d) Gostevskii, B.; Silbert, G.; Adear, K.; Sivaramakrishna, A.; Stalke, D.; Deuerlein, S.; Kocher, N.; Voronkov, M. G.; Kalikhman, I.; Kost, D. *Organometallics* **2005**, *24*, 2913−2920; and other articles in this series.

(15) Smith, P. H.; Kilroy, W. P.; James, S. D. *J. Chem. Eng. Data* **1984**, *29*, 284−285.

(16) (a) Mead, D. J.; Fuoss, R. M.; Kraus, C. A. *J. Am. Chem. Soc.* **1939**, *61*, 3257−3259. (b) Kraus, C. A.; Fuoss, R. M. *J. Am. Chem. Soc.* **1933**, *55*, 21−36.

(17) Karapetyan, Y. A.; Eychis, V. N. *Physico-chemical Properties of Non-aqueous Solutions of Electrolytes*; Khimia: Moscow, 1989.

(18) Rotinyan, A. L.; Tikhonov, K. I.; Shoshina, I. A. *Theoretical Electrochemistry*; Khimia: Leningrad, 1981.

(19) Jones, G.; Dole, M. *J. Am. Chem. Soc.* **1929**, *10*, 2950−2964.

(20) Falkenhagen, H.; Vernon, E. L. *Philos. Mag.* **1932**, *14*, 537−565.

(21) $\ln(f) = -AC^{1/2}/[1 + aBC^{1/2}]$ with, in CH_2Cl_2, $A = 13.636$ $L^{1/2}$ $mol^{-1/2}$ and $B = 9.834 \times 10^9$ $L^{1/2}$ $mol^{-1/2}$ m^{-1},[22] the interionic distance $a = (r_+ + r_s) + (r_- + 1.25r_s) = 10$ Å where r_+, r_-, and r_s are cation, anion, and solvent radii, respectively.[23,24]

(22) Damaskin, B. B.; Petrii, O. A. *Electrochemistry*; Vysshaia Shkola: Moscow, 1987.

(23) Kuznetsova, E. M.; Kirsanov, R. S. *Zh. Phys. Khim.* **1999**, *73*, 1776−1782.

(24) Kuznetsova, E. M. *Zh. Phys. Khim.* **2004**, *78*, 868−874.

(25) Fuoss, R. M. *J. Phys. Chem.* **1978**, *82*, 2427−2440.

(26) (a) Fuoss, R. M. *J. Phys. Chem.* **1985**, *89*, 3167−3173. (b) Fuoss, R. M. *Proc. Natl. Acad. Sci. U.S.A.* **1980**, *77*, 34−38.

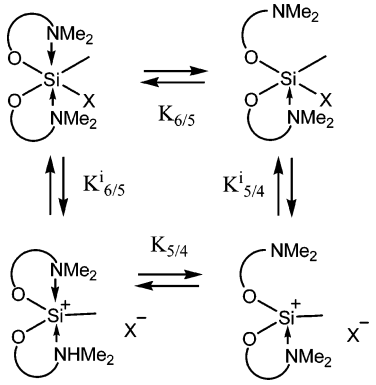

Figure 2. Schematic ionic and nonionic dissociation processes for **1**−**4**.

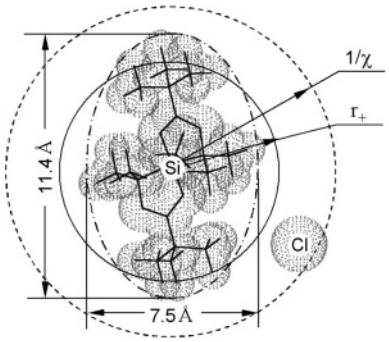

Figure 3. Ellipsoidal model of the cation of **1** calculated using the PM3 method,[27] with optimized geometry and its ion atmosphere radius (dotted line).

equilibrium $K^i_{5/4}$ shifts counterclockwise at higher T, in agreement with general considerations of conductivity in low-polar media.[3d,17,18,22] Ionic pentacoordinated species formed from a hexacoordinate dichelate through $K^i_{6/5}$ dissociation are supposed to be thermodynamically more stable than tetracoordinated ionic species obtained from dissociation with $K^i_{5/4}$ (preceded by nonionic dissociation with $K_{6/5}$). Hence even if these tetracoordinated species were formed, they would undergo an immediate stabilization by a pending hydrazide branch to end up as the same pentacoordinated ionized species. This latter species is therefore the only ionophore that might account for ionic conductance in this system.

Considering that the ionic 6/5 conversion involves Si−Cl bond elongation (Figure 3), the appearance of two distinct ions can be stated when this distance is at least $l_{Si...Cl} > r_+$. Therefore starting from $a = r_+ + r_-$ when the chemical bond Si−Cl obviously no longer exists, one can identify the species as a contact ion pair (second entity in eq 2). Larger solvent-separated ion pairs (third entity) exist from $a = r_+ + r_- + 2r_s$ up to Bjerrum critical distance r_{cr}, beyond which cations and anions behave independently.[3a]

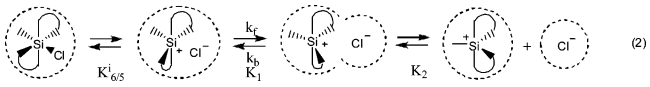

In general, the equilibrium with K_1 corresponds to ion motion from the Si···Cl distance in pentacoordinated species, freshly formed from $K^i_{6/5}$ interconversion, to the limiting ion-pair distance and covers all equilibriums between close, contact, and solvent-separated ion pairs. Provided that the rate of diffusion-controlled second-order reactions in CH_2Cl_2 is $k_d = 1.6 \times 10^{10}$ L mol^{-1} s^{-1},[28] it is hard to distinguish them by purely kinetic means. The time scale corresponding to this process can be roughly assessed through absolute ion mobilities u_{abs} and their linear drift velocities v:[3a] $t = (r_{cr} - l_{Si-Cl})/(v_+ + v_-) \ll 1$ ms. With K_2 being the ion-pair dissociation constant, the whole process is characterized by an apparent conductivity constant $K = 1/K_\Lambda = K^i_{6/5}K_1K_2$.

It can be seen from Table 1 that the formation of solvent-separated ion pairs can occur starting from the distance that is greater than 3 times the average Si−Cl bond length l_{Si-Cl}, $a = r_+ + r_- \cong 7$ Å, up to a minimal distance when the ions can show Stokes ionic conductivity in CH_2Cl_2, $r_{cr} = N_A|z_+z_-|e^2/(8\pi\epsilon_o\epsilon RT) \cong 31$ Å (e is the elementary charge, ϵ_o is the absolute dielectric permittivity).[18] The r_{cr} is almost 10 times larger than that for 1−1 ionophores in water ($r_{cr} = 3.57$ Å) and is substantially larger than the average size of cations of **1**−**4**.

The ion atmosphere radius, making up $1/\chi \approx 14$ Å at C_{min} for dichelates **1**−**3**,[29] rapidly increases with dilution, and already at $C \cong 0.9$ mmol L^{-1} it becomes longer than 31 Å, meaning that below this concentration Coulomb interactions are no longer strong enough to retain the ion pairs, which therefore dissociate. Due to the mobility of chelated silicenium ions and corresponding anions being high (see below and Table 1), molar conductivities then increase rapidly to converge to their limiting values.

To obtain information on the ion state in CH_2Cl_2 from experimental data, reliable data on limiting molar conductivities (λ^o, Λ^o) of the species concerned are needed. For dichelates **1**−**4**, the intercepts ($1/\Lambda_m{}^o$) of $1/\Lambda_m - \Lambda_m C$ plots extrapolated to $C \rightarrow 0$ are too close to zero, which does not allow determining correct $\Lambda_m{}^o$ values directly. They were therefore assessed as $\Lambda_m{}^\circ = \lambda_+{}^\circ + \lambda_-{}^\circ$ ($\lambda_+{}^\circ$ and $\lambda_-{}^\circ$ being limiting molar conductivities of the Si-centered cation and Cl$^-$ or TfO$^-$ anions resulting from dissociation of corresponding dichelates), with the entities on the right side, $\lambda_\pm{}^\circ$, calculated using different methods.

For Cl$^-$ and TfO$^-$, the λ° in many organic solvents are reported[17] so their λ° in CH_2Cl_2 can be estimated using Walden's rule.[31] For silicenium cations, no such data exist, so the corresponding values were first calculated using Stokes' equation (eq 3):[3a]

$$\lambda_+{}^o = N_A e^2/(6\pi\eta r_+) \qquad (3)$$

and then applying Kuznetsova's model[24] based on the concept that ion motion involves transient formation of a "hole" in the solvent and taking into account three degrees of freedom of translational motion of a complex ion in solution and local viscosity in the ion−solvent system (eq 4):[23]

$$\lambda^\circ = eFx/r_h\eta\{0.5y(y/x)^2[1 + r_s + 4r_s\sqrt{2}/(r + r_s)^2(1 + M_w/M_s)^{1/2}]\} \qquad (4)$$

(27) Beachy, M. D.; Cao, Y.; Murphy, R. B.; Perry, J. K.; Pollard, W. T.; Ringnalda, M. N.; Vacek, G. R.; Wright, J. R.; Deppmeier, B. J.; Driessen, A. J.; Hehre, W. J.; Johnson, J. A.; Klunzinger, P. E.; Watanabe, M.; Yu, J. *TITAN* release 1.07; Wavefunction, Inc., Schroedinger, Inc., 1999−2003.

(28) Atkins, P. W. *Chimie Physique*, 6th ed.; De Boeck University: Paris, 2000.

(29) Provided that for 1−1 ($z_+ = |z_-| = 1$) electrolytes $I = 0.5(C_+z^2_+ + C_-z^2_-) = C$, the Debye−Hückel length becomes $1/\chi = (10^3\epsilon_o\epsilon kT/2\pi e^2N_AC)^{1/2}$.[30]

(30) Bajin, N. M.; Ivanchenko, V. A.; Parmon, V. N. *Thermodynamics for Chemists*, 2nd ed.; Khimia: Moscow, 2004.

(31) The applicability of Walden's product $\lambda^\circ\eta$ for the estimation of $\lambda_{Cl}{}^\circ$ [3a] is somewhat contradictory since it is usually restricted to large ions ($r > 3$ Å).[32] For smaller Cl$^-$, it might introduce an additional error,[33] although the value obtained by this method ($\lambda_{Cl}{}^\circ = 103.2$ S cm^2 mol^{-1}) agrees rather well with that calculated from Stokes model ($\lambda_{Cl}{}^\circ = 110.3$ S cm^2 mol^{-1}).

Table 1. Radii of Ionic Species and Interionic Distances (Å) and Corresponding Limiting Ion and Molar Conductivities (S cm^2 mol^{-1}) for Dichelates 1−4

	r_+, Å	$\lambda_+°$ [a]	$\lambda_+°$ [b]	r_-, Å	$\lambda_-°$ [a]	$\lambda_-°$ [b]	$\Lambda_m°$ [a]	$\Lambda_m°$ [b]	a^{CIP}, Å [c]	a^{SSIP}, Å [c]
1	5.33	37.2	38.912	1.82	110.3	61.75	147.5	100.66	7.15	10.87
2	5.33	37.2	38.912	2.45	77.6	76.09	114.8	115.00	7.78	11.50
3	5.40	36.7	38.321	1.82	110.3	61.75	147.0	100.07	7.22	10.94
4	4.87	40.8	44.956	1.82	110.3	61.75	151.1	106.71	6.69	10.41

[a] From Stokes equation. [b]From Kuznetsova's model. For the anions studied, $y < 5.8$ Å ($r + 2r_s < x + 0.5r_h$);[23] therefore the monatomic model was used taking no account of the $(y/x)^2$ term in eq 4. [c]Superscripts CIP and SSIP at interionic distances *a* stand for close and solvent-separated ion pairs, respectively.

Table 2. Radii of Ionic Triples[a] (Å), Corresponding Conductivities[b] (S cm^2 mol^{-1}), and Equilibrium Constants for Dichelates 1−4 (eq 5)

cmpd	r_{+-+}, Å	$\lambda_{+-+}°$	r_{-+-}, Å	$\lambda_{-+-}°$	$\Lambda_T°$	Λ_{min} [c]	C_{min} [d]	K[e]	$1/K_\Lambda$	K_R [f]	K_S [f]	K_R [g]	K_S [g]
1	13.48	7.076	8.07	15.370	22.446	3	1.25	2.8×10^{-6}	7.1×10^{-6}	0.93	1.50×10^{5}	3.26	4.32×10^{4}
2	13.11	6.271	10.23	11.441	17.712	21	3.50	2.5×10^{-4}	4.1×10^{-5}	1.20	2.03×10^{4}	3.86	6.32×10^{3}
3	12.62	6.893	9.04	15.139	22.032	14	5.50	2.7×10^{-4}	3.3×10^{-5}	0.96	3.16×10^{4}	3.33	9.10×10^{3}
4	11.56	8.549	8.51	17.335	25.884	< 0.047	-	$< 1.5\times10^{-9}$	2.8×10^{-7}	0.76	4.70×10^{6}	2.87	1.24×10^{6}

[a] Ion triples masses for **1**−**4**, g mol^{-1}. (M_{+-+}): 693.5, 807, 777.5, 734.5; (M_{-+-}): 400, 627, 442, 420.5. [b]From Kuznetsova model with $r_{+-+} = 2r_+ + r_-$ and $r_{-+-} = r_+ + 2r_-$. For large ion triples, the frontal resistance of solvent molecules (r_s in denominator in eq 4) was neglected.[24] [c]From Λ_m corrected for solution viscosity. [d]*C*, 10^{-2} mol L^{-1}. [e]IP dissociation according to ref 4b. [f]For close ion pairs. [g]For solvent-separated ion pairs.

($\lambda°$ is in S cm^2 mol^{-1}, *x* is the mean distance between solvent molecules, r_h and r_s are the "hole" and solvent radii, respectively, *y* is the radius of the moving ionic complex $y = r + 1.25r_s$, M_w and M_s are the ion and solvent masses). The solvent radius r_s and the mean distance *x* were estimated from the solvent critical volume $V_{cr} = 12N_A(4\pi r_s^3/3)$ cm^3, and $x = (V/N_A)^{1/3} = (M_w/\rho N_A)^{1/3}$ m.[34] The "hole" size is given by $r_h = (8\pi/5)\text{-}(kT/\sigma)^{1/2}$ Å,[3a] where σ is the solvent surface tension, dyn/cm^2. The corresponding $\lambda_+°$ values are collected in Table 1.

Since the above model was developed for extreme cases—monatomic[23] or bulky[24] ions—its applicability for Cl^- and TfO^- was first tested on $[Bu_4N]ClO_4$ in CH_2Cl_2, the conductivity of the ClO_4^- anion being intermediate between those of Cl^- and TfO^-. Subtraction[35] of $\lambda°_{Bu_4N^+}$ (42.3 S cm^2 mol^{-1}) from $\Lambda°$ of this salt (109 S cm^2 mol^{-1})[37] provided the limiting conductivity of ClO_4^- ($\Lambda° - \lambda°_{Bu_4N^+} = \lambda°_{ClO_4^-} = 67$ S cm^2 mol^{-1}); direct calculation of $\lambda°_{ClO_4^-}$ according to Kuznetsova[23] yielded 67.768 S cm^2 mol^{-1}, which is a very good fit. The limiting conductivities of Cl^- and TfO^- in CH_2Cl_2 were calculated in a similar way (Table 1).

The values of $\Lambda_m°$ from the Stokes model seem to be overestimated, as they do not allow the convergence in any of the following procedures for conductivity fitting: Onsager−Fuoss,[3g] Fuoss-78,[25] and Fuoss-80/85.[26] In fact, the extrapolated molar conductivities of **1**−**4** converge well at about $C \cong 4.5 \times 10^{-6}$ mol L^{-1} to their $\Lambda_m°$ values calculated from Kuznetsova's model. Although this concentration seems rather high, it might be a good approximation for $C \rightarrow 0$. This is supported by the fact that for Bu_4NCl and Bu_4NSCN in CH_2Cl_2 this convergence occurs at $C \cong 4.9 \times 10^{-6}$ mol L^{-1},[33] which is surprisingly close to the above value.

Advanced theory of ionic conductance, which includes the effects of long-range interactions for virtual dipoles and dipolar ion pairs, was developed[26a] up to the concentrations $C_{max} \leq 0.2 \times 10^{-6} \times \epsilon^3$, which, for a 1−1 electrolyte at 25 °C, amounts to approximately 0.1 M for aqueous solutions but is limited to $C_{max} \leq 0.14 \times 10^{-3}$ mol L^{-1} in CH_2Cl_2. Obtaining reliable experimental conductivity data for extremely moisture sensitive silicon dichelates at these and even at 10-fold lower concentrations is a nontrivial task in itself (Figure 1). On the other hand, comparison of experimental Λ_m with theoretical values, calculated by a QBasic-written program, realizing the expansions developed by Fuoss,[25,26b,38] have shown that, in the considered interval of concentrations, convergence of an approximation with three fitting parameters and a concentration-dependent Debye term used beyond its upper limit proves insufficient.

Therefore, an estimation of equilibrium constants *K* has been made from an earlier model[4b,39] developed for cases of conductivity curves with a minimum (Table 2 lists the parameters for fitting the conductivity equation $\Lambda = \Lambda°K^{1/2}C^{-1/2} + \Lambda_T°(KC)^{1/2}K_T^{-1/2}$ where $\Lambda_T°$ and K_T are limiting conductivity and dissociation constant of ion triples). Dissociation constants ($K = 1/K_\Lambda$) for dichelates **2** and **3** are of the same order and about the same magnitude as the isodielectric constant obtained from general $\log(K) - \log(\epsilon)$ plot for CH_2Cl_2 ($K \cong 3 \times 10^{-4}$)[40] (cf. Bu_4NClO_4 in CH_2Cl_2, $K = 4.5 \times 10^{-5}$).[37] For **4** this value is substantially smaller.

Assuming these equilibrium constants to be a good first approach, at least for well-dissociated **2** and **3**, a combined treatment was applied to the conductivity data for **1**−**4**. Late Fuoss treatments,[25,26] based on the earlier Onsager−Fuoss algorithm[3g] with inclusion of $C^{3/2}$ terms, are limited in concentration by the ranges of interpolating polynomials. Therefore the latter model (regrouping the terms with different degrees of concentration) was used, which was completed by an empirical term $E(\alpha Cf)^{3/2}$ with *E* calibrated using known conductivity data in solvents with $\epsilon \cong 9$.[15,17,37,41,42]

(32) Barthel, J.; Wachter, R.; Gores, H. J. *Faraday Discuss. Chem. Soc.* **1977**, *64*, 285−294.
(33) Gill, D. S. *J. Chem. Soc., Faraday Trans.* **1981**, *77*, 751−758.
(34) Reed, R.; Sherwood, T. *Properties of Gases and Liquids*; Khimia: Leningrad, 1971.
(35) From the analysis of the ratio between ionic radius *r* and Δr of its solvate sphere, it was deduced[17] that the cations with $r > 3$ Å are not solvated even in strong donor solvents. However eq 4 provides a much better fit with the experiment when the thickness of the solvate shell is accounted for.[24,36] An additional reason for including the term r_s in *y* (eq 4) when calculating conductivities in generally noncoordinating CH_2Cl_2 is that the electrophilic Si in dichelates **1**−**4** has a large affinity for Cl; hence ion−solvent interactions cannot be neglected.
(36) Sigvarsten, T.; Gestblom, B.; Noreland, E.; Songstad, J. *Acta Chem. Scand.* **1989**, *43*, 103−115.
(37) Sun, H.; Biffinger, J. C.; DiMagno, S. G. *Dalton Trans.* **2005**, 3148−3154.
(38) Fuoss, R. M. *Proc. Natl. Acad. Sci. U.S.A.* **1978**, *75*, 16−20.
(39) Luder, W. F.; Kraus, P. B.; Kraus, C. A.; Fuoss, R. M. *J. Am. Chem. Soc.* **1936**, *58*, 255−258.
(40) Fuoss, R. M.; Kraus, C. A. *J. Am. Chem. Soc.* **1933**, *55*, 1019−1028.
(41) Romeo, R.; Arena, G.; Scolario, L. M.; Plutino, M. R. *Inorg. Chim. Acta* **1995**, *240*, 81−92.
(42) Danil de Namor, A. F.; Pugliese, A.; Casal, A. R.; Llerena, M. B.; Aymonio, P. J.; Velarde, F. S. *Phys. Chem. Chem. Phys.* **2000**, *2*, 4355−4360.

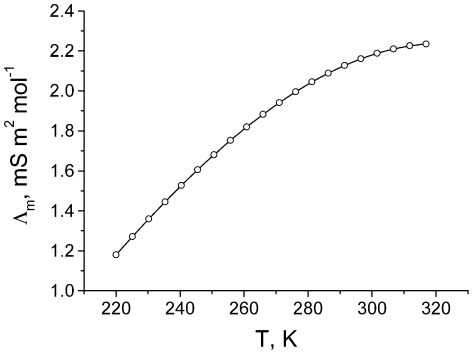

Figure 4. Molar conductivity of **2** (14 mmol/L in CH_2Cl_2) as a function of temperature.

Fuoss' model for ion pairing (eq 5, with γ as the fraction of free ions, $\gamma \rightarrow 0$, and α as the fraction of ion pairs A^+B^-)[25] is related to the equilibria in eq 2 through $K_R = 1/K_2$ and K_S being[43] $1/K_1$ or $1/K_1K^i_{6/5}$ (K_R is a solvent-specific and K_S is a substrate-dependent constant). The systems in consideration are

$$\underset{C\gamma}{A^+} + \underset{C\gamma}{B^-} \rightleftharpoons \underbrace{\underset{C(1-\gamma)(1-\alpha)}{A^+\cdots B^-} \rightleftharpoons \underset{C(1-\gamma)\alpha}{A^+B^-}}_{K_R} \left(\rightleftharpoons \underset{(1/K_1)\ K_S\ (1/K_{6/5})}{AB} \right) \tag{5}$$

at the upper concentration limit of Fuoss' model so $\alpha \cong 1$. The same follows considering $1/K = K_\Lambda = (1 - \alpha)/C\alpha^2f^2$ (f is a mean ion activity coefficient; $f \equiv 1$ for nondissociated ion pairs; $K_\Lambda = K_1/K_R$), which gives $\alpha > 0.98$ for all experimental K_Λ. On the other hand, equilibrium constants K_S can be assessed through $K_\Lambda = K_R(1 + K_S)$,[25] which, for actual α (i.e., when $K_S \gg 1$), is reduced to $K_\Lambda = K_RK_S$. The values of K_R were then estimated through $K_R = (4\pi N_A R^3/3000) \exp[\beta/a]$ (where β is the Bjerrum distance as $e^2/\epsilon_o\epsilon kT$)[3g] using the distance parameter a constructed in the hypothesis that large silicenium cations are not solvated and smaller anions are solvated according to Kuznetsova's model.[24] K_R and K_S obtained in this way for close and solvent-separated ion pairs are listed in Table 2.

Relative to other members of this series, dichelate **4** stays apart because of its very low conductivity and late minima on the $\Lambda_m - C$ curve. In the conductivity model based on Coulomb forces versus kinetic energy of thermal ion motion there is no specific physical reason for its conductance to be this different. In fact, once pentacoordinated and dissociated, the ions of all dichelates must behave similarly and show approximately similar K_R. Therefore, much weaker ionization of dichelate **4** (large K_S and $K^i_{6/5} \ll 1$) stems from a chemical reason.

Temperature Dependence of Conductivity

To provide insight into the thermodynamics of ion interactions in CH_2Cl_2, the temperature dependence of the molar conductivities of all dichelates was measured in the interval $-45 \le T \le 38$ °C. The Λ_m vs T graph for ionophore **2** shows a distinct trend to saturation at higher temperatures (Figure 4) with the conductivity maximum lying slightly above the solvent boiling point. Fifth degree polynomial extrapolation ($r = 0.9999$) located this maximum at 48 °C.

For dichelate **3**, also showing such maximum (Figure 5), a series of Λ_m vs T measurements at different concentrations revealed a negative shift of T_{max} for more diluted solutions. Explicit function $\Lambda_{max} = f(T, C)$ is quite complex,[44] but to a first approximation it appears close to linear on each parameter. It follows from Figure 5 that similar values of Λ_m are attained

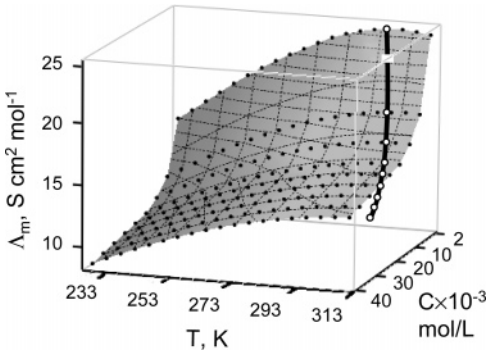

Figure 5. Temperature dependence of molar conductivity Λ_m of **3** in CH_2Cl_2 at different concentrations. With dilution, the maximum conductivity ($d\Lambda_m/dT|_c = 0$) is observed at lower temperatures (black line).

at lower concentrations as temperature decreases, which presumes negative ΔH^o of ion association. Applying the Gibbs–Helmholtz relationship[30] to K_S [obtained as above from $\Lambda(T) - C$ data for dichelate **3** (Figure 5)], this enthalpy was found to be $\Delta H°_{ass} = -5.11$ kJ mol^{-1}. Along with ΔG^o, it led to entropy of ion-pair formation, $\Delta S° = (\Delta H° - \Delta G°)/298 \approx 57-67$ J K^{-1} mol^{-1} (Table 3), which is very close to those ($\Delta S = 65-70$ J K^{-1} mol^{-1}) reported for poorly solvated Alk_4N^+ cations in *i*-PrOH.[3a]

In contrast to the generally negative $\Delta S°$ of cation–anion interactions, ion association entropies for **2** and **3** are positive, indicating that $\Delta S°$ of this process arises from solvent–solute restructuring, as was observed for the formation of contact ion pairs.[3a,45] The slightly lower values of $\Delta H°$ and $\Delta S°$ for dichelate **2** indicate that the TfO^- anion is less solvated in CH_2Cl_2 than Cl^-, in agreement with the assumptions made above for calculating $\lambda°_{Cl^-}$ and $\lambda°_{TfO^-}$.

For dichelate **1**, the Λ_m vs T graph reveals an opposite trend in the same temperature interval (Figure 6). Analysis of its first derivative and cautious polynomial inter/extrapolation indicate that the conductivity of **1** might have a maximum at lower temperatures corresponding to approximately $T_{max} = -110$ to -115 °C.

In contrast to other dichelates, the Λ_m vs T plot of **4** (Figure 7) shows three zones with different temperature coefficients of conductivity, with a negative value in the middle part. Physically, the conductivity of ionophores is reciprocal to solution viscosity and should therefore increase with temperature.[3a–d,44] Meanwhile, the sign of $d\Lambda_m/dT$ (or rather $d\kappa/dT$) is in general determined by the interplay between the activation enthalpy of solvent viscosity $\Delta H_\eta^\ddagger$ and the enthalpy of ion association, ΔH_{ass}[17,46] (eq 6),[47] since for low-polar solvents the third term on the right ($f' = f[R, d(\ln \rho)/d(1/T), d(1/\epsilon)/d(1/T)]$; ρ is the solution density) varies little with T:[17,44]

$$\Delta H_\kappa^\ddagger = \Delta H_\eta^\ddagger - (1/2)\Delta H_{ass} + f' \tag{6}$$

The conditions for observing a negative temperature coefficient usually involve large association constants K_{ass}. Indeed,

(43) The equilibrium in parentheses may or may not intervene depending on the coordination at silicon.

(44) (a) Bien, G. S.; Kraus, C. A.; Fuoss, R. M. *J. Am. Chem. Soc.* **1934**, *56*, 1860–1865. (b) Kuznetsova, E. M. *Zh. Phys. Khim.* **1999**, *73*, 2280–2282.

(45) (a) Tsurko, E. N.; Neueder, R.; Barthel, J. *J. Chem. Eng. Data* **2000**, *45*, 678–681. (b) Bester-Rogac, M.; Neueder, R.; Barthel, J. *J. Solution Chem.* **1999**, *28*, 1071–1086. (c) Bester-Rogac, M.; Babic, V.; Perger, T. M.; Neueder, R.; Barthel, J. *J. Mol. Liq.* **2005**, *118*, 111–118. (d) Schantz, S. *J. Chem. Phys.* **1991**, *94*, 6296–6306. (e) Chingakule, D. D. K.; Gans, P.; Gill, J. B.; London, P. J. *Monatsh. Chem.* **1992**, *123*, 521–535.

Table 3. Thermodynamic Parameters (ΔH and ΔG, kJ mol^{-1}; ΔS, J K^{-1} mol^{-1}) for the Ionic Conductivity of Dichelates 1−4

		CIP						SSIP					
cmpd	$\Delta H_\kappa^\ddagger$	$\Delta H°_{ass}$	$\Delta G°_{KS}$ [a]	$\Delta G°_{IP}$	$\Delta G°_{5/6}$	$\Delta S°_{IP}$	$\Delta S°_{5/6}$	$\Delta H°_{ass}$	$\Delta G°_{KS}$	$\Delta G°_{IP}$	$\Delta G°_{5/6}$	$\Delta S°_{IP}$	$\Delta S°_{5/6}$
1	−5.46	4.04	−29.28		−4.58		28.9	5.50	−26.00		−4.24		32.7
2	4.48	−3.19		−24.16		70.4		−3.18		−21.32		60.9	
3	4.38	−5.11		−25.24		67.6		−5.12		−22.21		57.4	
4	3.45[b]												
	−23.98	25.41	−37.43		−12.74		128.0	25.32	−34.18		−12.42		126.6
	2.78												

[a] Free enthalpy of ion association, $\Delta G° = -RT \ln(K_S)$. [b] For the corresponding linear parts of the $\ln(\Lambda_m \eta)$ vs $\ln(T)$ graph, see Figure 8.

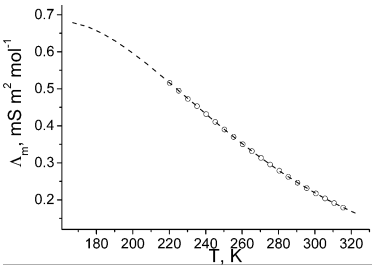

Figure 6. Molar conductivity of **1** (13.7 mmol/L) versus temperature in CH_2Cl_2. Dotted line corresponds to fifth degree polynomial inter/extrapolation of the experimental points.

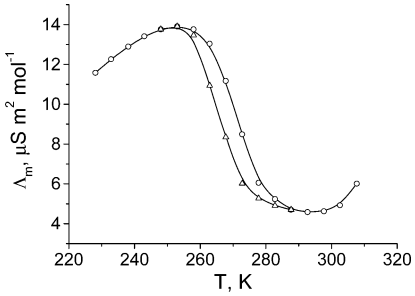

Figure 7. Conductivity of a 13.99 mmol/L solution of **4** in CH_2Cl_2 at different temperatures: (○) cooling pathway, (Δ) heating pathway. Experimental points are equally time spaced during the measurements.

this phenomenon has only been encountered for the salts with small anions and cations such as LiCl or $LiBF_4$, showing strong interionic interactions in low-ϵ solvents.[17,48] For larger species with a stable ionic character, e.g., Bu_4N^+ (small ΔH_{ass}), the temperature coefficients of conductivity are usually positive;[3a,17,49] therefore **1** and **4**, even bulkier compared to the cations of these salts, should seemingly follow this trend too. However, low η and ϵ promoting ion association are necessary, yet insufficient, requirement for the inversion of the $d\Lambda_m/dT$ sign. Additionally, there must be a substantial diminishing of ion concentration with the increase of temperature, which might result from interionic interactions or from other factors not accounted for in the Stokes model. The coordination lability of silicon and the prevalence of a nondissociated hexacoordinated form of **1** at higher temperatures and an extremely poor dissociation of **4** have the same effect as high ΔH_{ass} and can thus be responsible for the negative slope of their Λ_m vs T plots. Second inversion

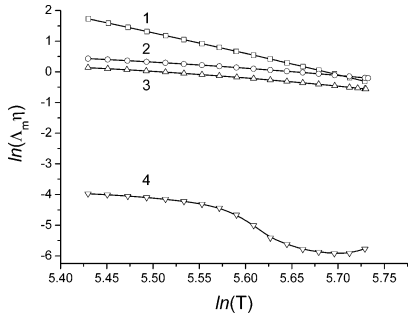

Figure 8. Temperature dependence of molar conductivity of dichelates **1**−**4** in CH_2Cl_2 corrected to variation of the solvent viscosity with temperature, η(T): (□) **1**, (○) **2**, (Δ) **3**, (▽) **4**.

of the $d\Lambda_m/dT$ sign for **4**, from negative to positive, at $T \geq 309-310$ K is probably due to the decrease of viscosity of CH_2Cl_2 when approaching its boiling point. Such a rise of conductivity is solely noticeable for weakly dissociated **4** ($d\Lambda_m \cong 2-3$ μS m^2 mol^{-1}) and is not seen for more conductive systems **1**−**3**, for which, with a conductivity $\Lambda_m \cong 200-2000$ μS m^2 mol^{-1}, the absolute value of this contribution amounts to only 0.1−0.2%.

As follows from the above analysis and from a ^{29}Si NMR chemical shift analysis,[2] dichelates **2** and **3** (and **4** at low T) behave as good ionophores whose Λ_m obeys the physical model of ionic conductivity and is not affected by coordination interconversion of Si. Their practically equal $\Delta\Lambda_m/\Delta\ln(T)$ values in Figure 8 are therefore "solvent slopes",[50] whereas larger slopes for **1** and **4** (its middle part) are of chemical origin and reflect a remarkable kinetic contribution to Λ_m.

Thanks to the additivity of thermodynamic functions, one can separate the contributions of different phenomena to K_S provided that $K_S = K_{IP}K_{5/6}$:

$$\Delta H(\Delta G)_{K_S}° = \Delta H(\Delta G)_{IP}° + \Delta H(\Delta G)_{5/6}° \qquad (8)$$

where the subscript IP relates to physical ion association ($1/K_\Lambda$ in eq 5). Assuming no contribution from $\Delta G_{5/6}°$ and $\Delta H_{5/6}°$ for **2** and **3** (for $\Delta G_{K_S}° = \Delta G_{IP}°$, it returns to the pure Fuoss−Onsager case,[3g] allowing the estimate of their values for **1** and **4** (Table 3).

$K_{5/6}$ for **1**, according to its Gibbs energy, equals 6.35 or 5.02 depending on whether close or solvent-separated ion pairs are formed. It is noteworthy that the value for close ion pairs gives practically the same equilibrium constant for 6/5 interconversion ($1/K_{5/6} = 0.157$) as that found for this dichelate from temperature-dependent ^{29}Si NMR measurements in CD_2Cl_2 ($K_{6/5} = 0.12$).[2]

A large positive entropic term for 5/6 interconversion of **4** stems from higher symmetry type and an additional valence

(46) Meurs, V. *Nature* **1958**, *29*, 1532−1533.

(47) Activation enthalpy of viscous flow in CH_2Cl_2 was estimated substituting the expressions of temperature dependence of its viscosity ($\eta = A \exp[-\Delta G_\eta^\ddagger/RT]$ with $A = 14.042 \times 10^{-3}$) and density ($\rho = (1.818-1.6825) \times 10^{-3}$ T) into eq 7 (h is Plank constant),[17] $\Delta G_\eta^\ddagger = RT \ln(\eta M_w/hN_A\rho)$ (7), and remembering that $\Delta H_\eta^\ddagger = d(\Delta G_\eta^\ddagger/T)/d(1/T)$; by differentiation of eq 7 one obtains $\Delta H_\eta^\ddagger = 6.78$ kJ mol^{-1}.

(48) (a) Barthel, J.; Gerber, R.; Gores, H. *Ber. Bunsenges. Phys. Chem.* **1984**, *N7*, 616−622. (b) Karapetyan, Y. A. *Ukr. Khim. Zhourn.* **1987**, *N5*, 483−486.

(49) Fuoss, R. *J. Am. Chem. Soc.* **1934**, *56*, 1857−1859.

(50) Higher values of $\Delta S°$ for close ion pairs compared to $\Delta S°$ of solvent-separated pairs (Table 3) also agree with solvent-driven association of these dichelates.

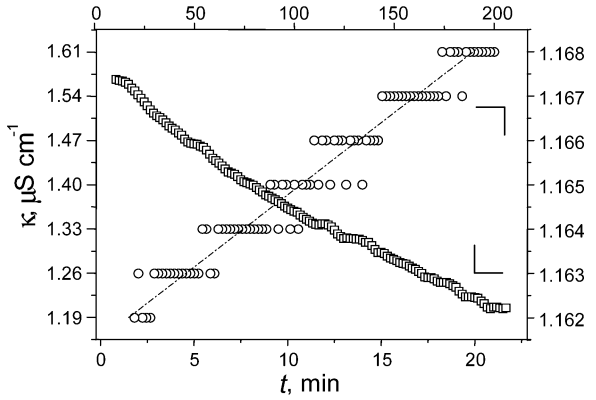

Figure 9. Time relaxation of specific conductivity of **4**: (□) heating direction, bottom and left scales; (○) cooling direction, upper and right scales. $T = 267.6$ K.

vibrational degree of freedom for this dichelate existing practically in one, hexacoordinated form. For **1**, this contribution is smaller, but still about 9 kJ mol^{-1} comes from the $T\Delta S$ term. The condition of eq 6 is obviously fulfilled for dichelates **2** and **3**, while larger association enthalpies for **1** and **4** invert the sign of $\Delta H_\kappa^{\ddagger}$. Therefore, once again, the physical model of conductivity applies for **2** and **3**, but it does not for **1** and **4**, because of substantial kinetic contribution to ΔH_{ass}.

Kinetic Aspect of Conductivity

It is interesting to note that the low- and high-temperature parts of the Λ_m vs T graph for **4** have practically the same "solvent-specific" slope and the activation energy as **2** and **3** (Figure 8), while its middle part shows the highest $\Delta H_\kappa^{\ddagger}$ in this series. The sigmoid shape of the Λ_m vs T plot arises from the fact that the association constant K_S for **4** is very large, and the formation of ionic species through 6/5 interconversion is very slow. The ionic pentacoordinated form is favored at low T, as is seen from higher Λ_m values. However at $T \leq 250$ K the time-averaged concentration of ions during the measurements remains almost unchanged, because of kinetic limitation of dissociation, so the Λ_m vs T graph reflects the conductivity of ions already present in solution, which is proportional to viscous flow in CH_2Cl_2, $1/\eta(T)$. Now its subsiding at lower T prevails over almost stopped increase in free ion concentration, causing the slope of the low-temperature part of the plot to regain the "solvent-specific" value.

This feature corroborates another remarkable distinction of **4** compared to **1**−**3**: for these three compounds cooling and heating patterns of the $\Lambda_m - T$ dependence are identical within the precision of measurements. For **4**, the low-temperature part also behaves in a similar way, while the part with the negative temperature coefficient (within $250 \leq T \leq 300$ K) reveals a distinct kinetic behavior and has different patterns depending on the direction it was plotted (Figure 7). In general, the conductivity is determined by ionic mobility $u_\pm$ of n carriers of the charge $z_\pm e$: $\kappa = z_\pm e\, n(u_+ + u_-)$. Provided that $C = n/N_A V$ and assuming ion mobility not to change within the interval of decay ($\approx 5\%$ of κ), the specific conductivity can be used as a direct image of concentration.[51] Thus, the time-dependent conductivity relaxation has shown (Figure 9) first- and second-order kinetics for the cooling and heating directions, respectively. A corresponding kinetic treatment of normalized dimensionless κ/κ_{fin} now allowed,[52] at a given T, estimating K_S via

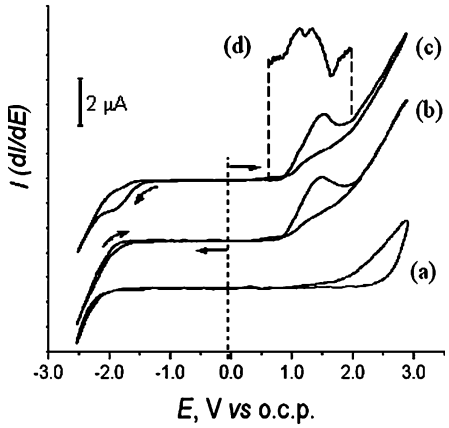

Figure 10. Voltammograms of **1** (9.16 mmol/L) at a Pt 5 mm diameter disk electrode in n-Bu_4NBPh_4 (45 mmol/L) solution in CH_2Cl_2: (a) baseline; (b) full scan starting from 0 V toward negative potentials; (c) full scan starting toward positive potentials; (d) first-derivative voltammogram of the oxidation peak showing two one-electron contributions. $\upsilon = 305.3$ mV/s; $T = 293$ K.

the apparent rate constants $k_f = k_f^{5/6} k_f^{IP}$ and $k_b = k_b^{5/6} k_b^{IP}$. Applying this procedure to different parts of the middle region of the $\Lambda(T)$ graph (Figure 7), the enthalpy ($\Delta H° = 23.07$ kJ mol^{-1}) and entropy ($\Delta S° = 121.1$ J K^{-1} mol^{-1}) of ion association were estimated from the slope ($\Delta H°/R$) and intercept ($-\Delta S°/R$) of van't Hoff's plot. For 298 K ($K_S = 4.08 \times 10^6$), subtracting, as above, $\Delta G_{IP}°$ from $\Delta G_{KS}°$ (-37.71 kJ mol^{-1}) yielded $\Delta G°_{5/6} = -13.01$ kJ mol^{-1}. Again, these data corroborate close ion-pair formation (Table 3).

Voltammetry of 1 in CH_2Cl_2 Solution

To avoid interference of strong commonly used anions such as BF_4^- and PF_6^- and to prevent the introduction of any F^- anions to the solution, a supporting salt with a bulky and soft anion, Bu_4NBPh_4, was used for voltammetric experiments. Dichelate **1** is not electroactive within the range of cathodic potentials down to the solvent reduction. In the anodic scan, it exhibits an oxidation peak that was shown by differential voltammetry to consist of two signals with similar potentials (Figure 10). When the scan is then continued in the cathodic direction, a well-shaped one-electron reduction signal appears before the solvent discharge. The limiting current i_p of this reduction peak has kinetic nature and depends on the scan rate (time elapsed between E_p^a and E_p^c when passing by anodic vertex potential). The half-life time of the species generated during the anodic period was estimated from $i_p - \upsilon$ experiments to be about $\tau_{1/2} \cong 67$ s at 20 °C.

The absolute electron stoichiometry of the process, determined from the $i_p \upsilon^{-1/2}$ to $it^{1/2}$ ratio in the same solution[53] provided $n = 1$ for both steps. Meanwhile, the n value obtained from comparison of the limiting currents i_p(**1**) with i_p of ferrocene at the same analytical concentration[54] only provided $n \cong 0.17$, which roughly corresponds to the percentage of the nondissociated hexacoordinated form of **1** at this temperature. It follows that this form accounts for the oxidation signal, which is in agreement with the conductivity measurements and ^{29}Si NMR data.[14c] The cathodic signal at E_p^c arises probably from the

(51) Salem, R. R. *Physical Chemistry. Thermodynamics*; Fizmatlit: Moscow, 2004.

(52) Emanuel, N. M.; Knorre, D. G. *Chemical Kinetics*, 4th ed.; Vysch. Shkola: Moscow, 1984.

(53) Malachesky, P. A. *Anal. Chem.* **1969**, *41*, 1493−1494.

(54) Taking no account of the difference in the diffusion coefficients of dichelate **1** and ferrocene.

reduction of a diazenium cation formed by oxidation of the hydrazide ligand in **1**.

The ionic pentacoordinated form of **1**, with the lone pairs of both hydrazide nitrogens involved in dative stabilization of the positively charged silicon, apparently has higher oxidation potential, which is beyond the solvent electrochemical window.

Conclusion

As follows from concentration- and temperature-dependent conductivity experiments, dichelates **2** and **3** behave as totally dissociated ionophores whose ion mobility increases with temperature as the solvent fluidity ($1/\eta$) increases. Their cations therefore exist in CH_2Cl_2 solution mostly as pentacoordinated N→Si←N dichelated silicenium ions, associated in close ion pairs with their counteranions. The conductivity of **1** reveals a dissociation pattern that is under kinetic control and that corroborates the increase of the amount of its pentacoordinated ionic form at lower temperatures. The same follows from cyclic voltammetry of this dichelate, revealing a labile equilibrium in CH_2Cl_2 solution. Contrary to its congeners, dichelate **4** is practically nondissociated, at least in low-polar CH_2Cl_2, and remains upon dissolution mostly in its hexacoordinated form. Both kinetic and thermodynamic considerations suggest that, in dichloromethane solutions, all ionized dichelates exist as ion pairs, most probably as close ones with a solvate shell common for the cation and anion.

The present electrochemical results are in complete harmony with the previously reported NMR analyses.[2b] We have shown here that **2** and **3** are essentially completely ionic compounds throughout the temperature range for which conductivities were measured. **2** has a triflate counterion, which is substantially less nucleophilic than chloride and, hence, shifts the ionic equilibrium (eq 1) completely to the right-hand side already at room temperature, as evident from its temperature-dependent ^{29}Si NMR spectral behavior.[2b] Likewise, it was shown previously that bulky monodentate ligands attached to silicon (**3**) push the equilibrium completely to the ionic side, already at room temperature.[2b] These results are now fully supported by the conductivity measurements, showing a "normal" increase of conductivity for **2** and **3** with decreasing solvent viscosity, as the temperature is increased.

The extent of ionization of **1** was previously shown to be strongly temperature dependent and driven by the solvent:[2b] ionization increased as the temperature was lowered, probably resulting from more intense hydrogen bonding of solvent molecules to the anion at lower temperatures (manifest in negative ionization entropy). As a result of this temperature dependence of dissociation of **1**, also the molar conductivity of **1** shows this unusual increase as the temperature decreases (Figure 6), due to the increase in ion concentration at lower temperature.

Finally, **4** stands out from the other complexes in its remarkably low conductivity (Figure 8). This is readily understood from previous results showing that **4** does not ionize at all in CD_2Cl_2 solution, because the presence of two strongly electronegative chloro ligands makes the silicon atom partly positively charged, and does not support formation of additional charge through ionic dissociation.

Experimental Section

Complexes **1**−**3** were reported previously.[2b]

Bis[*N*′-(dimethylamino)pivaloimidato-*N,O*]dichlorosilicon-(IV) (4). **4** was prepared in two steps, by chelate exchange of **1** with $SiCl_4$, as described recently.[55] A mixture of 1.207 g (5.58 mmol) of *O*-trimethylsilylated 1,1-dimethyl-2-pivaloylhydrazine[2b] and $MeSiCl_3$ (0.535 g, 3.58 mmol) in 5 mL of dry $CHCl_3$ was stirred for 1 h at room temperature. Removal of the volatiles under vacuum (0.05 mmHg) resulted in a colorless crystalline mass of **1**, which was used further without isolation. The crude **1** was dissolved in 10 mL of hexane, and to the solution was added by condensation $SiCl_4$ (0.507 g, 2.98 mmol). The mixture was stirred for 2 h at room temperature followed by removal of volatiles under vacuum (0.05 mmHg), leaving a colorless crystalline solid **4** (0.987 g, 92% over all yield). Mp: 110−110.5 °C. ^1H NMR ($CDCl_3$, 295 K): δ 3.02, 3.06 (2s, 12H, NMe_2), 1.07 (s, 18H, *t*-Bu). ^{13}C NMR ($CDCl_3$, 295 K): δ 26.7 ($C(CH_3)_3$), 35.0 ($C(CH_3)_3$), 51.9, 52.6 (NMe_2), 172.6 (C═N). ^{29}Si NMR ($CDCl_3$, 295 K): δ −147.1. Anal. Calcd for $C_{14}H_{30}Cl_2N_4O_2Si$: C, 43.63; H, 7.85; N, 14.54. Found: C, 43.51; H, 7.90; N, 14.72.

Conductivity measurements were carried out using a CDM-230 conductimeter (Radiometer Anal. SAS) with a 2-point probe. The cell was calibrated using a Bu_4NBPh_4/CH_2Cl_2 solution[56] and the measured data corrected to the residual solvent conductivity. Temperature-dependent conductivity measurements were performed on 13−15 mmol/L solutions of substrates in a 15 mL glass cell containing 12 mL of CH_2Cl_2 using a Huber CC156W Polystat CC2 cryogenic workstation and a 4-point Knick 703 conductimeter fitted with an internal thermocouple. The solvent was prepared by distilling anhydrous grade CH_2Cl_2 (Aldrich) over CaH_2 to a triply vacuum/argon (150 °C)-treated flask; the solvent was then transferred into the glovebox and filled with 3 Å molecular sieves activated at 350 °C during 3 days under the turbomolecular pump vacuum ($P = (5-6) \times 10^{-6}$ bar). Water content in the thus prepared solvent was checked by Karl Fischer titration to be below the sensitivity of the method. Water and oxygen content in the glovebox were <0.2 and <0.6 ppm, respectively.

To check the influence of residual moisture in the solvent, a conductivity curve of dichelate **2** was traced in CH_2Cl_2 containing $\sim 4.5 \times 10^{-4}$ mol L^{-1} water (Figure 1). Starting at the same Λ_m as in anhydrous CH_2Cl_2, the curve rapidly goes down to reach a minimum, after which the conductivity corresponds to that of triflic acid arising from total hydrolysis of **2**.

Voltammetric experiments were carried out in two-electrode mode using a homemade 12-channel potentiostat at a 5 mm diameter Pt disk electrode. Potentials were measured versus open circuit potential (ocp). Their conversion to the SCE scale can be done by the equation $E_{SCE}(V) = 0.635 \times E_{ocp} - 0.1$.

Acknowledgment. The authors are grateful to INTAS for financial support of this work (grant 03-51-4164), to the Israel Science Foundation (ISF 139/05), and to Dr. W. Kohs for access to the cryogenic workstation and assistance in the temperature-dependent conductivity measurements.

OM700687S

(55) Sergani, S.; Kalikhman, I.; Yakubovich, S.; Kost, D. *Organometallics* **2007**, *26*, xxxx−xxxx.

(56) Accascina, F.; Petrucci, S.; Fuoss R. M. *J. Am. Chem. Soc.* **1959**, *81*, 1301−1305.